Astrophys Space Sci (2015) 357:167
DOI 10.1007/s10509-015-2396-2

ORIGINAL ARTICLE

Evolution of the rotational motion of space debris acted upon by eddy current torque

Hou-Yuan Lin[1,2,3] · **Chang-Yin Zhao**[1,2]

Received: 23 January 2015 / Accepted: 18 May 2015 / Published online: 29 May 2015

Abstract Finding analytical solutions to the eddy current torque produced by a conducting body rotating within a magnetic field is arduous. In this paper, the finite difference method is adopted to solve numerically the boundary problem regarding the distributions of eddy currents in determining eddy current torque. Through analysis of the solutions, this paper presents the expression of eddy current torque that applies to a model of arbitrary shape rotating around an arbitrary axis. The parameters of the physical properties of the rigid body are integrated into the eddy current torque tensor, the features of which are analogous to the inertia tensor. The elements in the tensor are constants for a specific rigid body; thus, in the expression, the torque is associated only with the relative angular velocity and magnetic field. The expression is used to investigate the evolution of the rotation of space debris subjected to eddy current torque, through numerical integration with the angular velocity of the variation of the geomagnetic field, which is assumed a dipole. The results explain the observed phenomenon of change in the spin decay rate. Moreover, the effects of gravity-gradient torque and orbit precession cause the self-spin of the space debris to resonate with the orbital motion and ultimately, to reach a steady state.

Keywords Boundary problem · Eddy current torque · Rotational motion of space debris

✉ C.-Y. Zhao
cyzhao@pmo.ac.cn

[1] Purple Mountain Observatory, Chinese Academy of Sciences, Nanjing 210008, China

[2] Key Laboratory of Space Object and Debris Observation, PMO, CAS, Nanjing 210008, China

[3] University of Chinese Academy of Sciences, Beijing 100049, China

1 Introduction

It has been known since 1824 that any conducting body rotating within a magnetic field will slow down, but the exact formulation of this effect had no practical research application until the launch of the first artificial satellites (Wilson 1977). Nowadays, one of the key techniques in active debris removal from the space environment is to stabilize a non-cooperative rotational target and then to capture it (Liou 2011). Such a strategy requires thorough investigation of the effects of the geomagnetic field on the rotational state of space debris.

Eddy currents induced by a conducting body rotating within a magnetic field will interact with the field to produce torque. Eddy current torque not only decreases the spin speed but also precesses the spin vector (Smith 1965). The phenomenon that the angular velocity decays exponentially has been confirmed by observational data (Meeus 1971, 1974). Wilson (1959, 1977) fits the variations of the angular velocities of satellites to the inverse of the magnitude of the magnetic field, which is in good agreement with that of the geomagnetic field. Based on observational data, Williams and Meadows (1978) verified that eddy current torque is the primary factor in spin decay.

In early research into eddy current torque, the loop and spherical models are used. Subsequently, the models are developed into more complicated ones such as the cylinder and cone (Smith 1962) and even unique models for particular objects such as the Ariane upper stages (Praly et al. 2012). However, exact solutions have only been found for a sphere and spherical shell rotating within a uniform magnetic field (Halverson and Cohen 1964). The analytical expressions of the other models only apply to cases in which the object rotates around certain axes (e.g., the principal axis of inertia) and under limited conditions (e.g., the thin-wall case).

Numerous issues remain to be solved mainly because the boundary problem composed of Maxwell's electromagnetic field equations is intricate for such analytical solutions.

In this paper, the finite difference method is adopted to solve the boundary problem numerically in order to acquire the distributions of eddy currents, such that the eddy current torque can be derived. From the analysis of the numerical solutions, the expression of eddy current torque is presented in Sect. 2. This expression is appropriate for models with arbitrary shapes that rotate around their axes in any direction. In Sect. 3, the expression is used in a numerical integration to discuss the evolution of the rotation of space debris with consideration of the variation of the geomagnetic field in body-fixed system. The final rotational states under the effect of the geomagnetic field alone and when incorporating the additional effects of orbit precession and gravity-gradient torque are both presented.

2 Eddy current torque

The fundamental equations used to obtain the eddy current torque are introduced first. According to the law of electromagnetic induction, neglecting the transformer electromotive force, induced current density at position $\boldsymbol{r}$ relative to the center of mass can be expressed as (Smith 1962):

$$\boldsymbol{J} = \sigma\big(-\nabla\Phi + (\boldsymbol{\omega}\times\boldsymbol{r})\times\boldsymbol{B}\big), \tag{1}$$

where σ is the conductivity, Φ is the potential of the electric field, $\boldsymbol{\omega}$ is the rotational angular velocity of the rigid body relative to the magnetic field, and $\boldsymbol{B}$ is the magnetic field. The torque acting on unit volume $\mathrm{d}V$ of the rigid body relative to the center of mass is:

$$\mathrm{d}\boldsymbol{M} = \boldsymbol{r}\times(\boldsymbol{J}\times\boldsymbol{B})\mathrm{d}V. \tag{2}$$

Assuming steady state current density throughout, the distributions of the current density meet $\nabla\cdot\boldsymbol{J}=0$. Using Eq. (1) we attain:

$$\Delta\Phi = 2\boldsymbol{\omega}\cdot\boldsymbol{B}. \tag{3}$$

The boundary condition of the current density in the surface Γ of the rigid body is $\boldsymbol{J}\cdot\boldsymbol{n}=0$, where $\boldsymbol{n}$ is the normal of Γ. It is found that

$$\left.\frac{\partial\Phi}{\partial\boldsymbol{n}}\right|_{\Gamma} = \big((\boldsymbol{\omega}\times\boldsymbol{r})\times\boldsymbol{B}\big)\cdot\boldsymbol{n}. \tag{4}$$

Equations (3) and (4) simply define a Neumann problem (Praly et al. 2012). In this paper, the finite difference method is used to solve the Neumann problem to obtain the distributions of the current density and to derive the corresponding torque.

To present the expression of the general solution for eddy current torque, some particular solutions are listed beforehand. The magnetic field and instantaneous angular velocity of the rigid body relative to the magnetic field in the body-fixed coordinate system $OXYZ$ can be defined as $\boldsymbol{B}=(B_x,B_y,B_z)^{\mathrm{T}}$ and $\boldsymbol{\omega}=(\omega_x,\omega_y,\omega_z)^{\mathrm{T}}$, respectively. Then, under the assumption that the rigid body has uniform distribution, six independent torque values M_1–M_6 can be derived as particular solutions with particular angular velocities and magnetic fields:

$$\boldsymbol{M} = \begin{cases} \omega B^2(M_3,0,M_5)^{\mathrm{T}}, \\ \quad \text{when } \boldsymbol{\omega}=\omega(1,0,0)^{\mathrm{T}} \text{ and } \boldsymbol{B}=B(0,1,0)^{\mathrm{T}}, \\ \omega B^2(M_2,M_4,0)^{\mathrm{T}}, \\ \quad \text{when } \boldsymbol{\omega}=\omega(1,0,0)^{\mathrm{T}} \text{ and } \boldsymbol{B}=B(0,0,1)^{\mathrm{T}}, \\ \omega B^2(M_4,M_1,0)^{\mathrm{T}}, \\ \quad \text{when } \boldsymbol{\omega}=\omega(0,1,0)^{\mathrm{T}} \text{ and } \boldsymbol{B}=B(0,0,1)^{\mathrm{T}}, \\ \omega B^2(0,M_3,M_6)^{\mathrm{T}}, \\ \quad \text{when } \boldsymbol{\omega}=\omega(0,1,0)^{\mathrm{T}} \text{ and } \boldsymbol{B}=B(1,0,0)^{\mathrm{T}}, \\ \omega B^2(0,M_6,M_2)^{\mathrm{T}}, \\ \quad \text{when } \boldsymbol{\omega}=\omega(0,0,1)^{\mathrm{T}} \text{ and } \boldsymbol{B}=B(1,0,0)^{\mathrm{T}}, \\ \omega B^2(M_5,0,M_1)^{\mathrm{T}}, \\ \quad \text{when } \boldsymbol{\omega}=\omega(0,0,1)^{\mathrm{T}} \text{ and } \boldsymbol{B}=B(0,1,0)^{\mathrm{T}}, \end{cases} \tag{5}$$

where $\boldsymbol{M}=(M_x,M_y,M_z)^{\mathrm{T}}$ is the eddy current torque with respect to the center of mass. The torque with arbitrary angular velocity and magnetic field can be presented as the linear expression of M_1–M_6, which is written in matrix form as:

$$\boldsymbol{M} = \boldsymbol{B}\times\big(\boldsymbol{L}\cdot(\boldsymbol{\omega}\times\boldsymbol{B})\big), \tag{6}$$

where $\boldsymbol{L}$ is defined as the eddy current torque tensor:

$$\boldsymbol{L} = \begin{pmatrix} M_1 & -M_4 & -M_5 \\ -M_4 & M_2 & -M_6 \\ -M_5 & -M_6 & M_3 \end{pmatrix}. \tag{7}$$

The elements M_1–M_6 in the eddy current torque tensor are associated with the properties of the rigid body, e.g., the shape and conductivity. For a specific rigid body, these six variables are constants (small variations, such as the change of conductivity with temperature are neglected). Therefore, in the expression, the eddy current torque acting on the rigid body is related only to the instantaneous angular velocity and magnetic field. When the axes of the body-fixed coordinate system coincide with the principal axes of inertia (as mentioned above, the distribution of the rigid body is assumed uniform), the eddy current torque tensor can be reduced to a diagonal matrix, i.e., $M_4=M_5=M_6=0$, and the process is analogous to the diagonalization of the inertia tensor. According to Halverson and Cohen (1964), $M_1=M_2=M_3=2\pi\sigma r^4 d/3$ for a thin spherical shell, where r is the radius of the sphere, d is the thickness of the spherical shell, and $d\ll r$. For symmetrical models such as the cylinder and cone with the Z-axis along the center line, $M_1=M_2$. Therefore, when the rigid body rotates around the symmetric axis, i.e., $\omega_x=\omega_y=0$, the torque in Eq. (6) can be reduced to $\boldsymbol{M}=\kappa(\boldsymbol{\omega}\times\boldsymbol{B})\times\boldsymbol{B}$ (Smith 1962), where $\kappa=-M_1$.

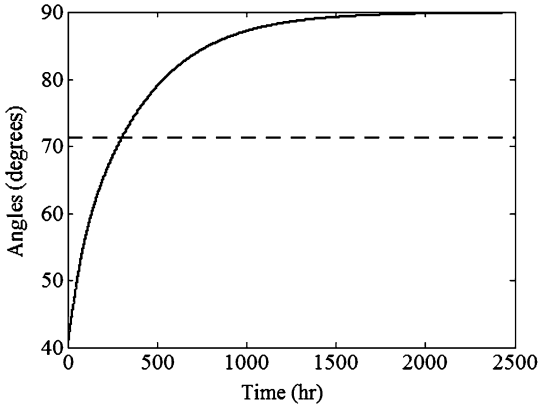

Fig. 1 Variation of the spherical coordinates of the angular momentum in the inertial system. The *dashed line* is the longitude of the angular momentum, which remains unchanged, the *solid line* is the latitude that gradually tends to 90°

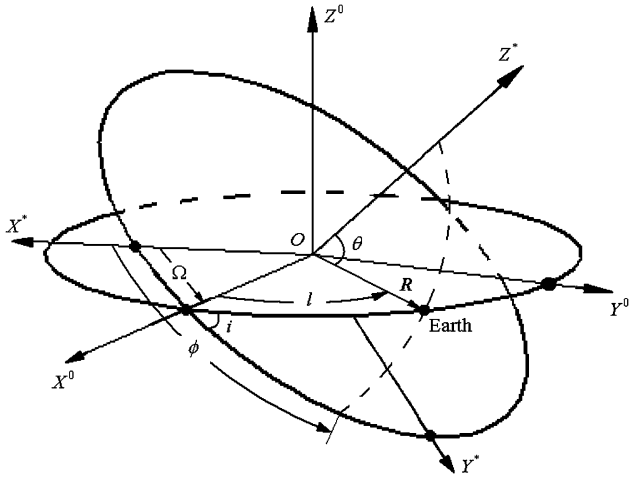

Fig. 2 Coordinate systems with their origins at the center of mass of the space debris. The $OX^*Y^*Z^*$ is translated from the inertial system whose fundamental plane is the equatorial plane of the Earth, and the OX^* axis points to the vernal equinox. The $OX^0Y^0Z^0$ is the orbit coordinate system of the space debris, and the OX^0 axis is in the direction of the ascending node. Ω is the longitude of the ascending node and i is the inclination of the orbit, $\boldsymbol{R}$ is the vector from the origin to the Earth, l is the angle between $\boldsymbol{R}$ and the OX^0 axis, and ϕ and θ are the azimuth and colatitude of $\boldsymbol{R}$ in the $OX^*Y^*Z^*$ system, respectively

3 Evolutions of rotational motion

3.1 Rotation within a uniform magnetic field

The expression of eddy current torque in Eq. (6) can be used in the numerical integration of the Euler dynamical equation described as

$$\boldsymbol{I}\dot{\boldsymbol{\omega}} + \boldsymbol{\omega} \times \boldsymbol{H} = \boldsymbol{M}, \tag{8}$$

where $\boldsymbol{I}$ is the inertia tensor and thus, the evolution of angular momentum can be obtained. An example in which the magnetic field is assumed uniform is shown in Fig. 1. Without loss of generality, the magnetic field $\boldsymbol{B}$ is chosen along the Z-axis of the inertial system. As shown in the figure, the longitude of the angular momentum remains unchanged in the long term but the latitude tends to 90°, which means that the angular momentum approaches the orientation of the magnetic field. Hence, it can be derived that the averaged eddy current torque is within the plane of the angular momentum and uniform magnetic field. As the torque is always perpendicular to the magnetic field (from Eq. (6)), the angular momentum moves gradually towards the direction (or the negative direction) of the magnetic field under the effect of the averaged eddy current torque.

3.2 Rotation of space debris within the geomagnetic field

3.2.1 Expressions of the geomagnetic field

For space debris, the uniform field only applies to the geomagnetic field for an orbit with near 0° inclination. The change of the geomagnetic field in body-fixed system during motion within the inclined orbit must be taken into account. To present the expressions of the geomagnetic field, two coordinate systems are established with origins at the center of mass of the space debris, as shown in Fig. 2. The $OX^*Y^*Z^*$ system is translated from the inertial system whose fundamental plane is the equatorial plane of the Earth, and the $OX^OY^OZ^O$ system is the orbit coordinate system. The longitude of the ascending node is Ω and the inclination of the orbit is i, $\boldsymbol{R}$ is the vector from the origin to the Earth in the orbital plane, l is the angle between $\boldsymbol{R}$ and the OX^O axis, and $\dot{l} = n$, where n is the mean motion rate.

In this paper, the geomagnetic field is approximated to a dipole field (Bertotti 1991) and the tilt of the magnetic dipole vector with respect to the spin axis of the Earth is neglected (Smith 1965). Thus, the geomagnetic field at the position of the space debris in the $OX^*Y^*Z^*$ system can be described as:

$$\boldsymbol{B} = \frac{s}{|\boldsymbol{R}|^3}\begin{pmatrix} -3\sin\theta\cos\theta\cos\phi \\ -3\sin\theta\cos\theta\sin\phi \\ 1-3\cos^2\theta \end{pmatrix}, \tag{9}$$

where s is the dipole strength, $s = 8 \times 10^{15}$ Wb·m for the Earth (Williams and Meadows 1978), ϕ is the azimuth starting from the OX^* axis, and θ is the colatitude. As shown in Fig. 2, ϕ and θ meet:

$$\begin{cases} \cos\theta = \sin i \sin l, \\ \tan(\phi - \Omega) = \cos i \tan l. \end{cases} \tag{10}$$

The angular velocity about the variation of the direction of the magnetic field cannot be ignored, especially in a situation where the space debris is rotating slowly. The angular velocity of the magnetic field vector in the body coordi-

nate system, expressed in the $OX^*Y^*Z^*$ coordinate system is $\boldsymbol{\omega}_B = \frac{\boldsymbol{B}\times\dot{\boldsymbol{B}}}{|\boldsymbol{B}|^2}$, where $\dot{\boldsymbol{B}}$ can be derived from Eq. (9) as:

$$\dot{\boldsymbol{B}} = n\frac{s}{|\boldsymbol{R}|^3}\begin{pmatrix} \frac{3\cos 2\theta \sin i\cos l\cos\phi}{\sin\theta} + \frac{3\sin 2\theta\cos^2(\phi-\Omega)\cos i\sin\phi}{2\cos^2 l} \\ \frac{3\cos 2\theta \sin i\cos l\sin\phi}{\sin\theta} - \frac{3\sin 2\theta\cos^2(\phi-\Omega)\cos i\cos\phi}{2\cos^2 l} \\ -6\cos\theta\sin i\cos l \end{pmatrix}. \tag{11}$$

Then, the angular velocity of the space debris with respect to the magnetic field is $\boldsymbol{\omega} = \boldsymbol{\omega}^* - \boldsymbol{\omega}_B$, where $\boldsymbol{\omega}^*$ is the angular velocity of the space debris in the $OX^*Y^*Z^*$ coordinate system.

3.2.2 Variation of angular velocity

The angular velocity of the space debris would decay exponentially under the effect of eddy current torque (Wilson 1959; Smith 1965), i.e., $\omega(t) = \omega_0 e^{-\lambda t}$, where ω_0 is the initial angular velocity, λ is the exponential decay rate, and t is the decay time. The rate of the exponential decay is associated with the magnitude of the magnetic field, shape of the space debris, conductivity, and moment of inertia, which are specific to the item of space debris. However, those with the same decay rate possess the same or similar evolutions, because the rate represents the effect of the eddy current torque acting on the space debris, which is independent of the initial angular velocity. In the numerical simulation here, the parameters are set to be close to reality. Thus, the model's moments of inertia in the three principal axes are 5×10^3, 4×10^3, and 1×10^3 kg·m^2, and the elements M_1–M_3 of the diagonalizable eddy current tensor are -2×10^5, -3×10^5, and -4×10^5 N·m^2·s/T^2. Thus, the decay rate of the angular velocity in the simulation is about 2 yr^{-1}, which is consistent with actual observational data (Wilson 1959, 1977; Meeus 1974). The orbit chosen in the simulation is the near-earth orbit and the eccentricity is near 0.

Using the Euler angles, the torque components given by Eq. (6) are expressed in the body coordinate system using the appropriate rotation matrices. The resulting Euler dynamical equations may then be integrated together with the orbital motion equations. The variation of angular velocity is shown in Fig. 3, in which the angular velocity decays exponentially under the effect of the geomagnetic field in the first 6 years, before it approaches a stationary value that is close to twice that of the mean motion rate. Note that during the exponential decay stage, the decay rate of the angular velocity has changed (see Fig. 3). This is because the angular velocity (and the angular momentum) shifts towards the axis of maximum inertia, following the dissipation of the eddy current torque after about 6 months when the space debris rotates around the non-principal axis. As shown in Fig. 4, angle θ_A between the angular velocity and the axis of maximum inertia tends to 0° after about 6 months and then it remains nearly stable. Furthermore, the angular velocity becomes aligned with the orientation of the axis of maximum inertia. The decay rates become different according to the change in the form of the eddy current torque expression.

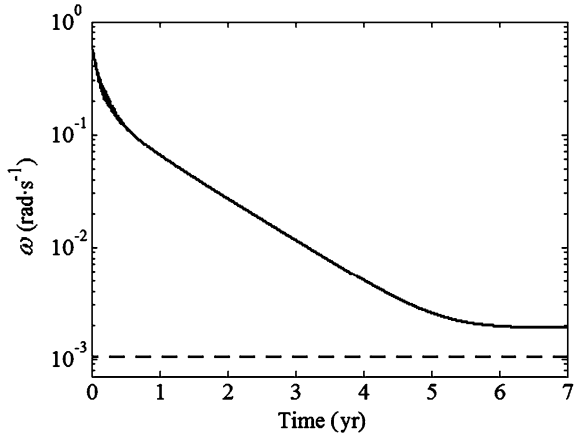

Fig. 3 Variation of the angular velocity versus time in an orbit with 800 km height and 70° inclination. The *solid line* is the variation of the angular velocity, the steady value of which after about 6 years is about 1.90×10^{-3} rad/s. The *dashed line* is the mean motion rate $n = 1.03\times10^{-3}$ rad/s

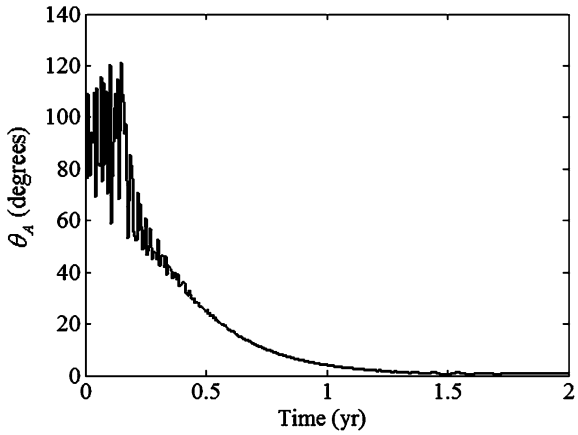

Fig. 4 Variation of angle θ_A between the angular velocity and axis of maximum inertia of the space debris

This result explains the same phenomenon of the observational data (Meeus 1974). It can be seen from Fig. 5 that the rotational decay rates of 1970-102B and 1971-13B both changed after about 6 months. It can be inferred that the nodes linking the different decay rates are the turning points of the rotations from around the non-principal axes to around the axes of maximum inertia.

3.2.3 Variations of angular momentum

The angular momentum of the space debris in the orbit coordinate system is described as

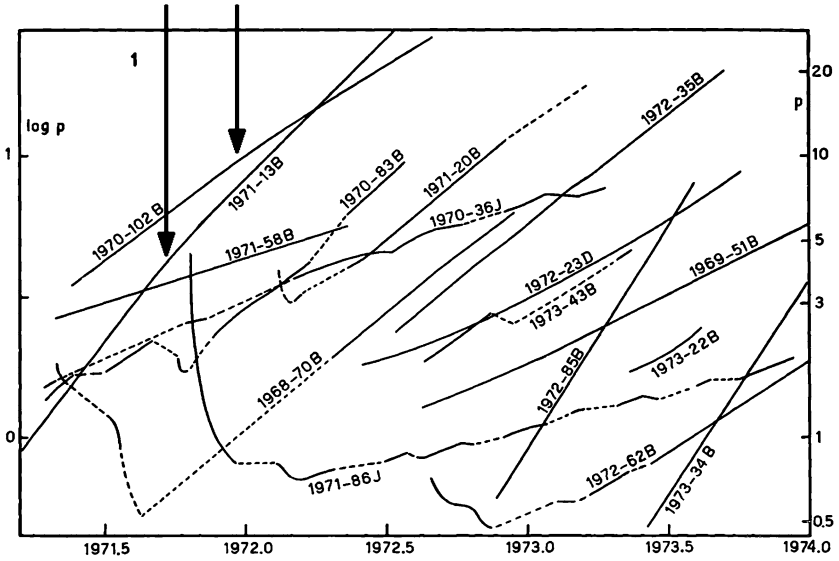

Fig. 5 Observational data of variations of the spin periods of rocket bodies, quoted from Meeus (1974) Fig. 1. The *arrows* denote the change points of the rotational decay rate (the slope) of 1970-102B and 1971-13B

$$\boldsymbol{H}^O = \begin{pmatrix} H_x^O \\ H_y^O \\ H_z^O \end{pmatrix} = |\boldsymbol{H}^O| \begin{pmatrix} \sin\psi_H \sin\theta_H \\ -\cos\psi_H \sin\theta_H \\ \cos\theta_H \end{pmatrix}, \tag{12}$$

where θ_H is the angle between the angular momentum and the OZ^O axis, and ψ_H is the longitude of $\boldsymbol{H}^O$ in the orbit coordinate system. The variations of six angular momentums whose initial values are chosen randomly are presented in Fig. 6.

From Fig. 6, it can be seen that all angular momentums ultimately turn into the same one, which is the stationary point marked by the dashed lines. However, the angular momentums do not move directly to the stationary point. Initially, because the angular velocity of the magnetic field could be neglected compared with the spin's high-speed, the directions of the magnetic fields in one orbital period could be averaged to a mean direction within the $Y^O Z^O$ plane (Smith 1965). Note that the average magnetic field direction is not the same as that of the axis of the dipole, because the object only samples a slice of the field along its orbit. Thus, the angular momentums approach the direction of the mean magnetic field (those numbered 2, 4, and 6 in Fig. 6) or its negative one (those numbered 1, 3, and 5 in Fig. 6), which is similar to that within the static uniform field (see Sect. 3.1).

When the angular velocities of the space debris decrease close to the magnitude of the geomagnetic field's angular velocity, the angular momentums of the space debris gradually shift to the stationary point, as is shown in Fig. 6(a) and (b). The stationary point of the angular momentums is associated with the distribution of the geomagnetic field, which is related to the orbit altitude and inclination (e.g., it is different between in Fig. 6(d) and (e) with different inclinations). This is also slightly sensitive to the physical properties of the space debris. The paths of the angular momentums toward the stationary point are different for different directions. From Fig. 6(c) and (d), the angular momentums numbered 1, 3, and 5, which approach to the negative direction of the mean magnetic field at the beginning, can move directly to the stationary point. However, those numbered 2, 4, and 6 approach from the opposite direction and encounter a barrier that they must bypass before arriving at the stationary point. The barrier only appears in the low inclination orbit after about 20 years, and its range narrows with increasing inclination. The barrier vanishes when the inclination is larger than about 45°, and then the angular momentums can move directly to the stationary point from both ends, as is shown in Fig. 6(e).

3.3 Evolutions under the additional effects

In Sect. 3.2, the evolutions of the rotational motion are only analyzed for an invariant orbit. However, the precession of an orbit due to the Earth's oblateness will alter the distribution of the magnetic field in the body-fixed system. Moreover, the gravity-gradient torque cannot be ignored when the angular momentum is small. Therefore, the orbit precession and gravity-gradient torque are added to the numerical simulation to analyze the evolutions of the rotational motion further. Using the same parameters as in Fig. 3, the variations of the angular velocity and θ_H are plotted in Fig. 7. It is found that in about the first 4.5 years, the variation of angular velocity is similar to that without the gravity-gradient torque. This is because the magnitude of the gravity-gradient torque is small and it has no long-term effect on the angular momentum. The early oscillation of θ_H arises from the orbit precession. Then, when the angular velocity decreases to a certain value (after about 4.5 years in Fig. 7), the space debris enters an attitude adjustment phase that lasts for months. The angular velocity and θ_H change wildly during the attitude adjustment phase. The duration of this phase is associ-

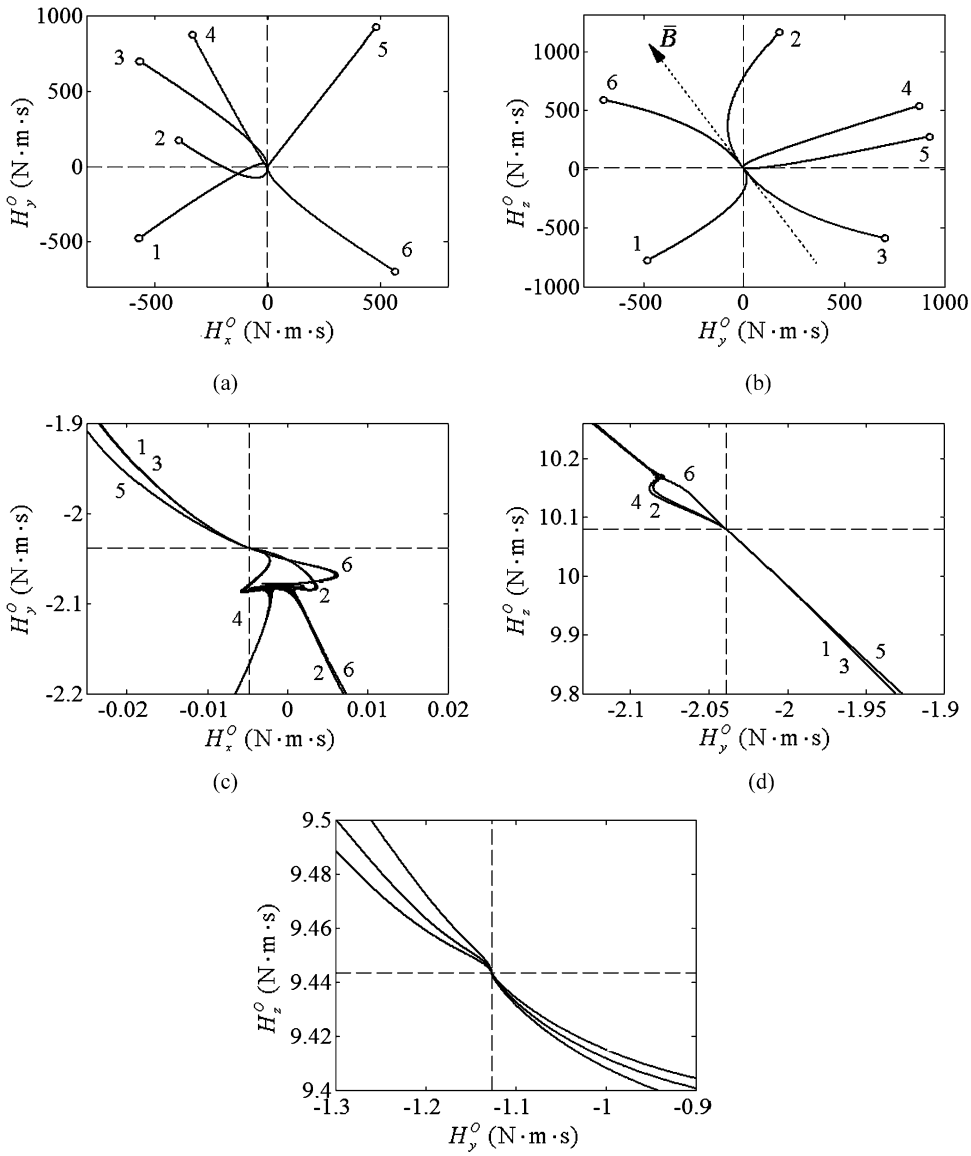

Fig. 6 Variations of angular momentums in the orbit coordinate system: (**a**) and (**b**) are the projections of angular momentums on the $X^O Y^O$ and $Y^O Z^O$ planes, respectively, in a near-circular orbit at 800 km height and 30° inclination; (**c**) and (**d**) are enlarged views of (**a**) and (**b**) around the stationary point, respectively; (**e**) is the same view as (**d**) for an orbit with 70° inclination. The *six solid lines*, numbered 1–6, denote the evolutions of different initial rotational states. The *hollow circles* are the initial angular momentums. The intersection of the *dashed lines* marks the stationary point at the end of the evolutions. The *dotted line* in (**b**) is the approximate direction of the averaged magnetic field $\bar{\boldsymbol{B}}$ through the origin, which is within the $Y^O Z^O$ plane

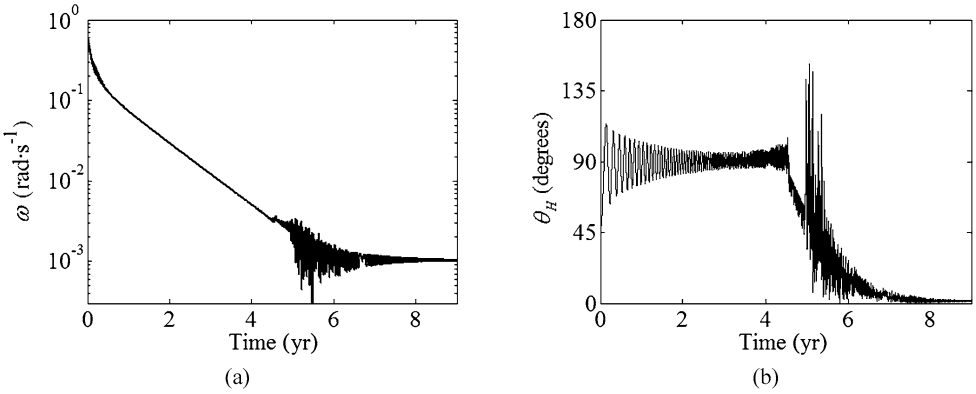

Fig. 7 (**a**) and (**b**) are the angular velocity and angle θ_H between the angular momentum and the normal of the orbital plane, respectively, as functions of time with the gravity-gradient torque and orbit precession taken into account

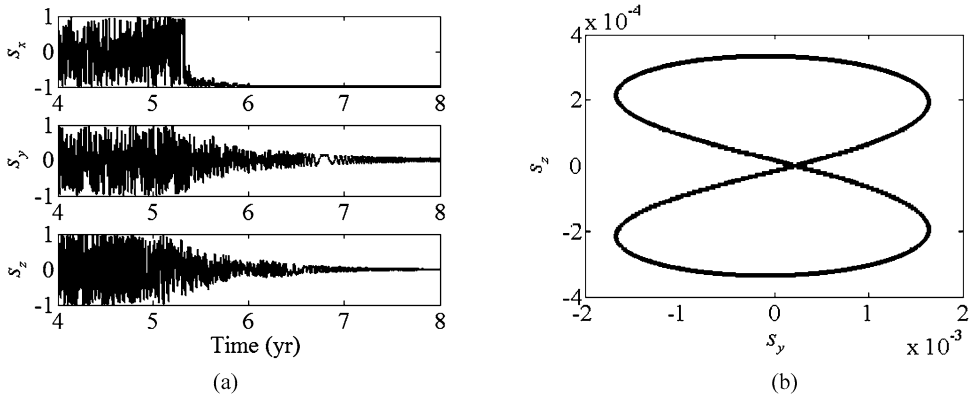

Fig. 8 (**a**) is the variation of the three components of the unit vector $\boldsymbol{s} = (s_x, s_y, s_z)^{\mathrm{T}}$ along the axis of minimum inertia in the rotating coordinate system. It can be seen that the rotation enters the resonant phase after about 5.3 years; (**b**) is the terminal state of components s_y and s_z after about 15 years, which are two linked closed curves

ated with the initial rotational state. Subsequently, a 1:1 resonance develops between the rotational motion and orbital motion, and the angular velocity vibrates around the mean motion rate n. During the resonant phase, the amplitude of the angular velocity decreases gradually and the angular velocity itself approaches the mean motion rate. The angular momentum also gradually tends toward the normal of the orbital plane.

To analyze the attitude motion of the space debris relative to the Earth during the resonant phase, a rotating coordinate system $OX^{\mathrm{r}}Y^{\mathrm{r}}Z^{\mathrm{r}}$ is built with the orbital plane being the fundamental plane and $\boldsymbol{R}$ being the X^{r}-axis. The unit vector along the axis of minimum inertia in the rotating coordinate system is defined as $\boldsymbol{s} = (s_x, s_y, s_z)^{\mathrm{T}}$, the variations of which are shown in Fig. 8(a). In the resonant phase, the axis of minimum inertia is constrained to one side of the X^{r}-axis, i.e., it points (or is contrary) to the Earth throughout, and s_y and s_z change disorderly within the vibration ranges. The vibration ranges of the components decrease over time and they eventually achieve stability. The stable trajectory of $\boldsymbol{s}$ in the $Y^{\mathrm{r}}Z^{\mathrm{r}}$ plane consists of two linked symmetric curves, as shown in Fig. 8(b). It is obvious that the shapes and sizes of the curves are not definite, because they are sensitive to the eddy current torque and gravity-gradient torque acting on the space debris.

4 Conclusions

In this paper, the finite difference method is used to solve the boundary problem regarding the distributions of eddy currents, from which the eddy current torque can be obtained. Through analysis of the solutions, an expression of the eddy current torque is presented that can be applied to models with arbitrary shapes rotating around an arbitrary axis. In the expression, the parameters of the properties of the rigid body are integrated into a tensor, which is called the eddy current torque tensor. The features of the eddy current torque tensor are analogous to those of the inertia tensor. The elements in the tensor are constants for a specific rigid body, which means the torque in the expression is associated only with the relative angular velocity and magnetic field. Hence, it can facilitate research on the effects of the eddy current torque.

Using the expression, the evolutions of the rotation of the rigid body under the effects of the eddy current torque are obtained through numerical integration. Within a uniform magnetic field, the angular momentum of the rigid body gradually tends to the direction (or the negative direction) of the magnetic field. For the conducting space debris in orbit, the evolutions of the rotations are achieved through simulations with the angular velocity of the variation of the geomagnetic field, which is assumed a dipole. The results explain the observed phenomenon of change in the spin decay rate. Moreover, the combined effects of gravity-gradient torque and orbit precession cause the self-spin of the space debris to resonate with the revolution and ultimately, to reach a steady state.

Acknowledgements This research was supported by the National Science Fund for Distinguished Young Scientists of China (Grant no. 11125315). We wish to thank Dr. Ojakangas for his helpful comments on this paper.

References

Bertotti, B.: The rotation of LAGEOS. J. Geophys. Res. **96**, 2431–2440 (1991)

Halverson, R., Cohen, H.: Torque on a spinning hollow sphere in a uniform magnetic field. Aerosp. Navig. Electron. **ANE-11**, 118–122 (1964)

Liou, J.-C.: An active debris removal parametric study for LEO environment remediation. Adv. Space Res. **47**, 1865–1876 (2011)

Meeus, J.: Satellites artificiels—Observations de périodes photométriques 1968–1971. Ciel Terre **87**, 606 (1971)

Meeus, J.: Satellites artificiels—observations de périodes photométriques, 1971–1973. Ciel Terre **90**, 201 (1974)

Praly, N., Hillion, M., Bonnal, C., Laurent-Varin, J., Petit, N.: Study on the eddy current damping of the spin dynamics of space debris from the Ariane launcher upper stages. Acta Astronaut. **76**, 145–153 (2012)

Smith, G.: A theoretical study of the torques induced by a magnetic field on rotating cylinders and spinning thin-wall cones, cone frustums, and general body of revolution. In: NASA TR R-129, pp. 1–20 (1962)

Smith, G.: Effects of magnetically induced eddy-current torques on spin motions of an earth satellite. In: Nasa TN D-2198 (1965)

Williams, V., Meadows, A.J.: Eddy current torques, air torques, and the spin decay of cylindrical rocket bodies in orbit. Planet. Space Sci. **26**, 721–726 (1978)

Wilson, R.H.: Magnetic damping of rotation of satellite 1958β2. Science **130**, 791–793 (1959)

Wilson, R.H.: Magnetic effects on space vehicles and other celestial bodies. Ir. Astron. J. **13**, 1–13 (1977)